

Theory of Sodium, Magnesium, and Aluminum

WALTER A. HARRISON

General Electric Research Laboratory, Schenectady, New York

(Received 12 June 1964)

A theory relating the electronic structure and the properties of metals has been described earlier. It was based upon the self-consistent-field method and a perturbation solution of the energy-band calculation. This theory is now applied explicitly to Na, Mg, and Al. The orthogonalized plane wave (OPW) form factors and the energy-lattice wave-number characteristic were computed by machine and used to compute atomic properties. The correct metallic structure was found to have lowest energy in each case: hcp, hcp, and fcc, respectively. Computed c/a ratios for sodium and magnesium of 1.63 and 1.62, respectively, are close to those observed. The elastic shear constant for axial distortions was computed for the hexagonal phase of each metal; for magnesium the constant is known and the agreement excellent. The vibration spectrum for fcc aluminum is computed and corresponds to errors in the elastic constants of the order of a factor of 2; this sensitivity reflects strong cancellation (which greatly increases from sodium to aluminum) between electrostatic and band-structure contributions to the energy. Calculations of the total binding energy of aluminum and the variation of energy with lattice parameter are quite inaccurate. Inclusion of a free-electron exchange and correlation correction does not significantly improve the results and, in fact, makes the crystal unstable against the formation of lattice distortions. Pressure dependence of the elastic constants was calculated for aluminum and gave discrepancies of a factor of 2. It is concluded that the theory gives a rather good account of changes in energy due to ion rearrangement at constant volume, but not of changes in energy due to changes in volume. A phenomenology is proposed in which the pseudopotential is adjusted to fit the observed vibration spectrum. This phenomenology is applied to aluminum with a single adjustable parameter and the resulting energy-lattice wave-number characteristic given.

I. INTRODUCTION

IN two earlier papers^{1,2} we developed a method for calculating most of the properties of simple metals from first principles and this scheme was applied to zinc. In essence this was a scheme for carrying out a band calculation, but was carried out in a perturbation approximation which permitted the treatment of general arrangements of the ions. Furthermore, because of the perturbation treatment, it was possible to treat directly many electronic properties and even to sum the total energy as a function of the position of ions and thereby to treat atomic properties. Agreement with experiment with respect to electronic properties was very good, and we have subsequently obtained and published³ the characteristics which determine the electronic properties for all nontransition metals with atomic number less than that of zinc.

With respect to the atomic properties, the situation was less clear. The energy-wave-number characteristic which determines the atomic properties was obtained for zinc by hand calculation and was clearly not accurate enough to give a quantitative check on the theory; in some cases reasonable agreement was obtained, in other cases not. We have therefore embarked upon a machine calculation to test the theory with respect to atomic properties. A program was written which reads the Hartree-Fock wave functions and parameters for the core, and also reads the atomic volume. It then produces the energy-wave-number characteristic, as well as other interesting curves. The same program was applied to

sodium, magnesium, and aluminum and a number of properties treated. The present paper describes these results.

The method used is essentially that given earlier, but some improvements in the formulation and in the numerical approximations have been made. In addition, volume-dependent terms are included. It seems desirable to outline the theory from the start rather than to list all of the modifications which are made. This will also enable us to illuminate the relation of the pseudopotential method to the orthogonalized plane wave (OPW) method and the difference between different pseudopotentials in what seems to the author as a lucid way. This is certainly not the only manner in which such comparisons may be made; Pick and Sarma⁴ as well as Bassani and Celli,⁵ Austin, Heine and Sham,⁶ and Cohen and Heine⁷ have given general discussions of the pseudopotential method.

Three important physical approximations enter the theory.

(1) The self-consistent-field approximation. We include exchange between conduction and core electrons in a Slater⁸ free-electron approximation though full Hartree-Fock exchange could be used with little additional effort. In the main body of the paper interactions between conduction electrons were treated in the Hartree approximation. Some calculations also were carried out and reported in Sec. VI in which exchange

¹ W. A. Harrison, *Phys. Rev.* **129**, 2503 (1963).

² W. A. Harrison, *Phys. Rev.* **129**, 2512 (1963).

³ W. A. Harrison, *Phys. Rev.* **131**, 2433 (1963).

⁴ R. Pick and G. Sarma, *Phys. Rev.* **135**, A1363 (1964).

⁵ F. Bassani and V. Celli, *Phys. Chem. Solids* **20**, 64 (1961).

⁶ B. J. Austin, V. Heine, and L. J. Sham, *Phys. Rev.* **127**, 276 (1962).

⁷ M. H. Cohen and V. Heine, *Phys. Rev.* **122**, 1821 (1961).

⁸ J. C. Slater, *Phys. Rev.* **81**, 385 (1951).

and correlation were included in a free-electron approximation which is a straightforward extension of Slater's free-electron exchange suggested by Brooks.⁹ A somewhat different correction for correlation and exchange based upon Hubbard's¹⁰ method has been used by Sham¹¹ in treating the vibration spectrum of sodium.

(2) The cores are treated as small. This approximation enters in three different ways. First, overlap of adjacent ions is neglected so that the only direct ion-ion interaction is through the Coulomb fields. Second, the variation over the core of the fields due to adjacent ions and due to the conduction electrons is neglected. Thus, the core wave functions (though clearly not the core energies) are the same as in the isolated ion. The validity of this assumption can be readily verified by noting that the core functions are almost identical in the ion and in the atom. Third, in the evaluation of integrals of the products of core functions and various slowly varying functions, the slowly varying functions are evaluated at the nucleus and taken out of the integral. For the metals we treat these approximations are very good. However, this assumption is important in limiting the metals which we may treat; in particular, the noble and transition metals are ruled out.

(3) A perturbation method for solution of the OPW method carried to second order. The perturbation expansion is by no means unique; we intend to clarify our expansion early in the formulation. The expansion appears reasonable on the grounds that the matrix elements which enter are generally small (of the order of a tenth) in comparison to the Fermi energy. A further qualitative check on the expansion is made by computing the valence-electron charge density in the atomic cell. For the face-centered cubic structure the charge density is found to be quite uniform, suggesting that deviations from single-plane-wave behavior might reasonably be treated as a perturbation. Of course part of the purpose for our treatment of these metals is to see from experiment to what extent this second-order theory is adequate.

II. FORMULATION

We will restrict our treatment to the calculation of energy eigenstates; in our earlier analysis¹ we formulated also time-dependent calculations. Thus we will begin by writing the time-independent Schrödinger equation which is satisfied by the one-electron wave functions ψ_k ,

$$H\psi_k = [T + V(\mathbf{r})]\psi_k = E_k\psi_k. \quad (1)$$

Here H is the Hamiltonian. T is the kinetic energy, $-\hbar^2\nabla^2/2m$, and $V(\mathbf{r})$ is the self-consistent potential including Slater free-electron exchange between conduction and core electrons.

We next distinguish between electronic core states

(subscript α) and conduction-band states (subscript \mathbf{k}). According to our second assumption above, the core wave functions ψ_α are the same as in the isolated ion, though the core energies E_α will be different from that in the ion.

$$H\psi_\alpha = E_\alpha\psi_\alpha. \quad (2)$$

The subscript α denotes the position of the ion in the metal as well as the angular-momentum and energy quantum numbers.

The conduction-band states are to be expanded in orthogonalized plane waves; that is, plane waves which have been orthogonalized to every core state on every atom wherever that atom may lie. It is convenient to abbreviate our notation by using the projection operator P introduced by Pick and Sarma.⁴ P projects any function on the core wave functions; thus, an orthogonalized plane wave may be written

$$e^{i\mathbf{k}\cdot\mathbf{r}} - \sum_\alpha \psi_\alpha(\mathbf{r}) \int \psi_\alpha^*(\mathbf{r}') e^{i\mathbf{k}\cdot\mathbf{r}'} d\tau' \equiv (1-P)e^{i\mathbf{k}\cdot\mathbf{r}}. \quad (3)$$

It is convenient to normalize our plane waves in the volume of the crystal Ω . We write such normalized plane waves and normalized core functions in the form,

$$|\mathbf{k}\rangle = \Omega^{-1/2} \exp i\mathbf{k}\cdot\mathbf{r}, \quad (4)$$

$$|\alpha\rangle = \psi_\alpha(\mathbf{r}). \quad (5)$$

Using the notation of Eqs. (3), (4), and (5), we may write explicitly the expansion of the wave function ψ_k in orthogonalized plane waves.

$$\psi_k = \sum_{\mathbf{q}} a_{\mathbf{q}}(\mathbf{k})(1-P)|\mathbf{k}+\mathbf{q}\rangle. \quad (6)$$

We may substitute this form in the Schrödinger equation [Eq. (1)] and rearrange terms to obtain

$$\sum_{\mathbf{q}} a_{\mathbf{q}}(\mathbf{k})T|\mathbf{k}+\mathbf{q}\rangle + \sum_{\mathbf{q}} a_{\mathbf{q}}(\mathbf{k})[V + (E_k - H)P]|\mathbf{k}+\mathbf{q}\rangle = E_k \sum_{\mathbf{q}} a_{\mathbf{q}}(\mathbf{k})|\mathbf{k}+\mathbf{q}\rangle. \quad (7)$$

Simply by arranging terms in this way we have taken the pseudopotential point of view. We note that Eq. (7) has the form

$$T\phi_k + W\phi_k = E_k\phi_k \quad (8)$$

with

$$\phi_k = \sum_{\mathbf{q}} a_{\mathbf{q}}(\mathbf{k})|\mathbf{k}+\mathbf{q}\rangle \quad (9)$$

and

$$W = V + (E_k - H)P = V + \sum_{\alpha} (E_k - E_{\alpha})|\alpha\rangle\langle\alpha|. \quad (10)$$

Thus we have defined a nonlocal pseudopotential W which we treat as a perturbation. In a more straightforward OPW calculation we would have left all E_k terms on the right-hand side and developed a secular equation for evaluating the eigenvalue E_k . In the pseudopotential method the eigenvalue, at least at this stage, appears also in the pseudopotential itself.

We may note at this point a peculiarity in the pseudopotential method. Cohen and Heine⁷ and Bassani and

⁹ H. Brooks, *Trans. AIME* **227**, 546 (1963).

¹⁰ J. Hubbard, *Proc. Roy. Soc. (London)* **A243**, 336 (1958).

¹¹ L. J. Sham (to be published).

Celli⁵ have noted that any linear combination of core wave functions may be added to ϕ_k and it will remain a solution of Eq. (8) and will lead to the same wave function ψ_k as derived by Eq. (6). Austin, Heine, and Sham⁶ have further pointed out that W may be replaced by a general pseudopotential,

$$W\phi_k = V\phi_k + \sum_{\alpha} \langle f(\mathbf{r}, \alpha) | \phi_k \rangle | \alpha \rangle, \quad (11)$$

where $f(\mathbf{r}, \alpha)$ is an arbitrary function of position and of core index α , and Eq. (8) will have solutions of the same eigenvalues E_k . The arbitrariness in $f(\mathbf{r}, \alpha)$ and in ϕ_k is the same; a particular $f(\mathbf{r}, \alpha)$ leads to a unique ϕ_k unless W is taken with the specific form of Eq. (9), the latter being valid for all ϕ_k . By selecting a particular set of solutions ϕ_k , we may select a particular form for the pseudopotential W and thereby eliminate the dependence of W upon E_k ; this is done without approximation. At the same time we may attempt to select a ϕ_k which will optimize the convergence of the perturbation expansion. Thus we at once eliminate the ambiguity, remove the dependence of W upon the eigenvalue, and in some sense optimize the convergence.

It is convenient to develop the perturbation expansion before specifying the form of W . We regard W as a first-order quantity and in the standard way obtain the first-order coefficients of the expansion of the wave function and the energy to second order.

$$a_q(\mathbf{k}) = \frac{\langle \mathbf{k} + \mathbf{q} | W | \mathbf{k} \rangle}{(\hbar^2/2m)(k^2 - (\mathbf{k} + \mathbf{q})^2)} a_0(\mathbf{k}). \quad (12)$$

$$E_k = \frac{\hbar^2 k^2}{2m} + \langle \mathbf{k} | W | \mathbf{k} \rangle + \sum_q \frac{\langle \mathbf{k} | W | \mathbf{k} + \mathbf{q} \rangle \langle \mathbf{k} + \mathbf{q} | W | \mathbf{k} \rangle}{(\hbar^2/2m)(k^2 - (\mathbf{k} + \mathbf{q})^2)}. \quad (13)$$

The first-order wave functions based upon Eq. (12) will be used to compute the self-consistent screening field.

In order to select the form of the pseudopotential, we may write the general pseudopotential of Eq. (11) as applied to a plane wave $|\mathbf{k}\rangle$. This is done by making a Fourier expansion of $f(\mathbf{r}, \alpha)$; the result may be written in the form,

$$W|\mathbf{k}\rangle = V|\mathbf{k}\rangle + \sum_{\alpha} f(\mathbf{k}, \alpha) |\alpha\rangle \langle \alpha | \mathbf{k}\rangle. \quad (14)$$

For each choice of the arbitrary function $f(\mathbf{k}, \alpha)$, we will obtain a particular form for the pseudo wave function ϕ_k . Whatever form we choose, we will use the single plane $|\mathbf{k}\rangle$ as the zero-order approximation to ϕ_k . Thus a reasonable criterion might be based upon taking a form such that ϕ_k is as close as possible to a plane wave. To obtain this in terms of a criterion for $f(\mathbf{k}, \alpha)$, we note that W operating on any true pseudo wave function ϕ_k must give $V\phi_k + \sum_{\alpha} (E_k - E_{\alpha}) |\alpha\rangle \langle \alpha | \phi_k\rangle$. If $|\mathbf{k}\rangle$ is to be close to the true ϕ_k corresponding to a given form of Eq. (14), then $f(\mathbf{k}, \alpha)$ must be close to $E_k - E_{\alpha}$. We are

therefore motivated to select the best value of E_k from Eq. (13) short of requiring an iteration for the determination of W and we obtain the form

$$W|\mathbf{k}\rangle = V|\mathbf{k}\rangle + \sum_{\alpha} \langle \hbar^2 k^2 / 2m + \langle \mathbf{k} | W | \mathbf{k} \rangle - E_{\alpha} \rangle |\alpha\rangle \langle \alpha | \mathbf{k}\rangle. \quad (15)$$

Replacing \mathbf{k} by \mathbf{k} in the right-hand side would also be a possible choice, but would make W non-Hermitian. (*Note added in proof.* Such a choice leads to the same energies to second order.) In these terms the pseudopotential of Bassani and Celli⁵ corresponds to taking $f(\mathbf{k}, \alpha)$ equal to $\hbar^2 k^2 / 2m + \langle \mathbf{k} | V | \mathbf{k} \rangle - E_{\alpha}$; that of Pick and Sarma,⁴ to taking $f(\mathbf{k}, \alpha)$ equal to $\hbar^2 k^2 / 2m - E_{\alpha}$; and the simple plane-wave expansion of ψ_k , to taking $f(\mathbf{k}, \alpha)$ equal to zero. It should be mentioned again that all four forms are valid pseudopotentials.

We may also show¹² that the form of Eq. (15), is precisely the one that we obtained earlier^{1,13} by following the procedure given by Cohen and Heine⁷ for selecting the ϕ_k which is the smoothest; that is, the ϕ_k having a minimum $(\nabla\phi_k, \nabla\phi_k) / (\phi_k, \phi_k)$. This latter procedure is certainly the better defined, and possibly the more convincing argument supporting the particular pseudopotential which we use. We will not, however, repeat that argument, but proceed with the form of Eq. (15).

The evaluation of matrix elements of W from Eq. (15) is not straightforward. We have the considerable problem of sorting out the contributions to the self-consistent potential V from the ions and the electrons, and also in determining the values of E_{α} in the metal. A discussion of these problems is relegated to the Appendix, where we develop explicit expressions for the matrix elements of W and evaluate the total energy.

In the course of these calculations the matrix elements of W and of P are factored as in diffraction theory. There is a form factor which is a matrix element for a single ion and is independent of the positions of the ions; these form factors are written $\langle \mathbf{k} + \mathbf{q} | w | \mathbf{k} \rangle$ and $\langle \mathbf{k} + \mathbf{q} | p | \mathbf{k} \rangle$ and enter directly in calculations of electronic properties.^{1,2} There is also a geometrical structure factor $S(\mathbf{q})$ given by

$$S(\mathbf{q}) = (1/N) \sum_j \exp(-i\mathbf{q} \cdot \mathbf{r}_j), \quad (16)$$

where the sum is over all N ion positions \mathbf{r}_j . This is precisely the structure factor which enters diffraction theory.

The energy is finally divided into three terms. First is a free-electron energy E_{fe} which depends upon the atomic volume but is otherwise independent of the arrangements of the ions. Second is a band-structure energy given by

$$E_{bs} = \sum_q' S(\mathbf{q})^* S(\mathbf{q}) E(q), \quad (17)$$

¹² This is most readily done by noting that $(\hbar^2 k^2 / 2m - E_{\alpha}) |\alpha\rangle \langle \alpha | \mathbf{k}\rangle = |\alpha\rangle \langle \alpha | T - H | \mathbf{k}\rangle = -PV | \mathbf{k}\rangle$.

¹³ W. A. Harrison, Phys. Rev. **126**, 497 (1962).

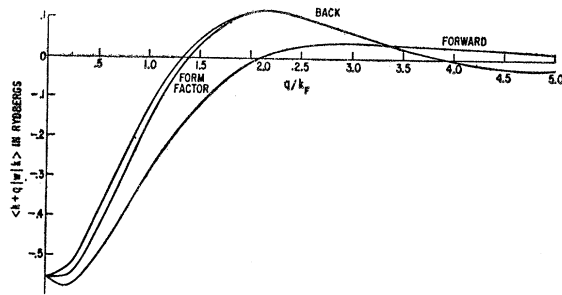


FIG. 1. Matrix elements of the pseudopotential for aluminum. \mathbf{k} is taken to lie on the Fermi surface; for forward scattering \mathbf{q} lies parallel to \mathbf{k} ; for back scattering \mathbf{q} lies antiparallel to \mathbf{k} ; the form factor gives matrix elements for $\mathbf{k} + \mathbf{q}$ lying on the Fermi surface.

where $E(q)$ is called the energy-wave-number characteristic; it depends upon the atomic volume and the local potentials but is independent of the detailed ion positions. $E(q)$ may be thought of as the change in energy due to the introduction of a Brillouin-zone plane corresponding to a lattice-wave-number \mathbf{q} . The prime on the sum indicates that the $\mathbf{q} = 0$ term is excluded. Finally there is an electrostatic energy which is the energy of point ions of effective valence

$$Z^* = Z(1 + (NZ)^{-1} \sum_k \langle \mathbf{k} | \rho | \mathbf{k} \rangle) \quad (18)$$

embedded in a uniform compensating background. This effective charge is the same as that given by Pick and Sarma⁴ and differs from that we used earlier due to a slightly different decomposition of the total energy.

III. CALCULATIONS AND RESULTS

The procedure described in the last section and in the Appendix was programmed for a GE 225 computer for elements in the third row of the periodic table. The program reads the atomic volume, the valence, the Hartree-Fock wave functions for the $1s$, $2s$, and $2p$ functions in the isolated ions and their corresponding Hartree-Fock energies. It then computes $E(q)$, and other interesting curves.

The many integrals to be performed are carried out numerically, generally using Simpson's rule. For real-space integrals the interval was given by that for the tabulated wave function. Reciprocal-space integrals were based upon intervals in wave-number space of $0.1k_F$. Additional care was taken where principal values of integrals were required. Integrals over the Fermi sphere showed cylindrical symmetry, so the numerical volume integration involved sums over circles; over 200 circles in the Fermi sphere were used, these being packed more closely where the circles were longer.

Hartree-Fock cores were taken for sodium from Hartree and Hartree,¹⁴ for magnesium from Yost,¹⁵ and

for aluminum from Froese.¹⁶ The atomic volumes used were those observed and are 267, 154, and 111.4 a. u. (or Bohr radii cubed) for Na, Mg, and Al, respectively.

In the course of the $E(q)$ calculation, the form factors $\langle \mathbf{k} + \mathbf{q} | w | \mathbf{k} \rangle$ of the matrix elements are computed; these are the matrix elements of the pseudopotential associated with a single ion. Figure 1 shows a set of such matrix elements for aluminum for \mathbf{k} lying on the Fermi surface and for \mathbf{q} parallel to and antiparallel to \mathbf{k} . If the pseudopotential could be replaced by a local potential, these curves would be identical. As we found earlier for zinc,² these curves differ greatly, particularly in the important region $q = 1.5k_F$ to $q = 2k_F$. The use of the true nonlocal pseudopotential would appear to be quite important in aluminum as well as zinc. Similar curves for sodium and magnesium indicate the same variations.

Also shown on Fig. 1 is the OPW form factor for aluminum; this is the matrix element between two states both of which lie on the Fermi surface. This is the curve which determines many electronic properties, as we found earlier.^{1,2} In Table I we have tabulated the OPW form factors for sodium, magnesium, and aluminum. These differ by less than 0.02 Ry from the cruder curves we obtained earlier³ by hand.

The main result of our calculations is the energy lattice-wave-number characteristic, $E(q)$, which determines the band-structure energy according to Eq. (17). These are tabulated for the observed atomic volume in Table II along with the parameter

$$\langle \mathbf{k} | \rho | \mathbf{k} \rangle_{av} = (NZ)^{-1} \sum_k \langle \mathbf{k} | \rho | \mathbf{k} \rangle,$$

which determines the effective valence of Eq. (18) determining the electrostatic energy. The final column will be discussed in Sec. VII. The $E(q)$ curves of Table II are displayed in Fig. 2. The peak near $2k_F$ arises because of

TABLE I. OPW form factor $\langle \mathbf{k} + \mathbf{q} | w | \mathbf{k} \rangle$ in rydbergs.

q/k_F	Sodium	Magnesium	Aluminum
0.1	-0.5551
0.2	-0.1464	-0.3424	-0.5524
0.3	-0.1458	-0.3320	-0.5272
0.4	-0.1392	-0.3094	-0.4837
0.5	-0.1333	-0.2858	-0.4369
0.6	-0.1293	-0.2632	-0.3901
0.7	-0.1229	-0.2361	-0.3378
0.8	-0.1134	-0.2043	-0.2810
0.9	-0.1041	-0.1732	-0.2265
1.0	-0.0954	-0.1439	-0.1763
1.1	-0.0852	-0.1137	-0.1274
1.2	-0.0731	-0.0828	-0.0805
1.3	-0.0615	-0.0546	-0.0393
1.4	-0.0495	-0.0280	-0.0024
1.5	-0.0379	-0.0041	+0.0288
1.6	-0.0272	+0.0162	0.0543
1.7	-0.0162	0.0346	0.0755
1.8	-0.0060	0.0500	0.0915
1.9	+0.0038	0.0626	0.1031
2.0	0.0130	0.0728	0.1107

¹⁴ D. R. Hartree and W. Hartree, Proc. Roy. Soc. (London) A193, 299 (1948).

¹⁵ W. J. Yost, Phys. Rev. 58, 557 (1940).

¹⁶ C. J. Froese, Proc. Camb. Phil. Soc. 53, 210 (1957).

TABLE II. Energy-wave-number characteristic $E(q)$ in rydbergs per electron. The effective valence for electrostatic energy is $Z^* = Z(1 + \langle k|p|k \rangle_{av})$.

q/k_F	Sodium $\langle k p k \rangle_{av} = 0.0750$	Magnesium $\langle k p k \rangle_{av} = 0.0850$	Aluminum $\langle k p k \rangle_{av} = 0.0790$	Aluminum (Phenomenological) $\langle k p k \rangle_{av} = 0.0790$
0.1	-2.178×10	-3.572×10	-4.515×10	-4.509×10
0.2	-5.371	-8.648	-1.081×10	-1.075×10
0.3	-2.332	-3.641	-4.470	-4.418
0.4	-1.266	-1.894	-2.267	-2.220
0.5	-7.724×10 ⁻¹	-1.093	-1.267	-1.224
0.6	-5.038×10 ⁻¹	-6.671×10 ⁻¹	-7.425×10 ⁻¹	-7.057×10 ⁻¹
0.7	-3.416×10 ⁻¹	-4.176×10 ⁻¹	-4.430×10 ⁻¹	-4.119×10 ⁻¹
0.8	-2.362×10 ⁻¹	-2.629×10 ⁻¹	-2.633×10 ⁻¹	-2.378×10 ⁻¹
0.9	-1.646×10 ⁻¹	-1.639×10 ⁻¹	-1.533×10 ⁻¹	-1.331×10 ⁻¹
1.0	-1.144×10 ⁻¹	-9.999×10 ⁻²	-8.597×10 ⁻²	-7.066×10 ⁻²
1.1	-7.853×10 ⁻²	-5.857×10 ⁻²	-4.529×10 ⁻²	-3.428×10 ⁻²
1.2	-5.256×10 ⁻²	-3.218×10 ⁻²	-2.160×10 ⁻²	-1.430×10 ⁻²
1.3	-3.399×10 ⁻²	-1.608×10 ⁻²	-8.782×10 ⁻³	-4.546×10 ⁻³
1.4	-2.091×10 ⁻²	-6.930×10 ⁻³	-2.746×10 ⁻³	-9.309×10 ⁻⁴
1.5	-1.200×10 ⁻²	-2.353×10 ⁻³	-6.996×10 ⁻⁴	-7.001×10 ⁻⁴
1.6	-6.217×10 ⁻³	-6.270×10 ⁻⁴	-7.744×10 ⁻⁴	-2.057×10 ⁻³
1.7	-2.724×10 ⁻³	-5.448×10 ⁻⁴	-1.759×10 ⁻³	-3.839×10 ⁻³
1.8	-9.053×10 ⁻⁴	-1.241×10 ⁻³	-2.887×10 ⁻³	-5.352×10 ⁻³
1.9	-2.003×10 ⁻⁴	-2.067×10 ⁻³	-3.657×10 ⁻³	-6.159×10 ⁻³
2.0	-1.474×10 ⁻⁴	-2.483×10 ⁻³	-3.655×10 ⁻³	-5.849×10 ⁻³
2.1	-3.564×10 ⁻⁴	-2.504×10 ⁻³	-3.222×10 ⁻³	-5.011×10 ⁻³
2.2	-6.605×10 ⁻⁴	-2.514×10 ⁻³	-2.907×10 ⁻³	-4.405×10 ⁻³
2.3	-9.580×10 ⁻⁴	-2.432×10 ⁻³	-2.577×10 ⁻³	-3.826×10 ⁻³
2.4	-1.202×10 ⁻³	-2.279×10 ⁻³	-2.244×10 ⁻³	-3.277×10 ⁻³
2.5	-1.378×10 ⁻³	-2.080×10 ⁻³	-1.920×10 ⁻³	-2.769×10 ⁻³
2.6	-1.484×10 ⁻³	-1.861×10 ⁻³	-1.620×10 ⁻³	-2.314×10 ⁻³
2.7	-1.529×10 ⁻³	-1.638×10 ⁻³	-1.350×10 ⁻³	-1.914×10 ⁻³
2.8	-1.524×10 ⁻³	-1.421×10 ⁻³	-1.112×10 ⁻³	-1.568×10 ⁻³
2.9	-1.481×10 ⁻³	-1.220×10 ⁻³	-9.067×10 ⁻⁴	-1.273×10 ⁻³
3.0	-1.410×10 ⁻³	-1.037×10 ⁻³	-7.322×10 ⁻⁴	-1.026×10 ⁻³
3.1	-1.322×10 ⁻³	-8.752×10 ⁻⁴	-5.863×10 ⁻⁴	-8.212×10 ⁻⁴
3.2	-1.223×10 ⁻³	-7.331×10 ⁻⁴	-4.658×10 ⁻⁴	-6.528×10 ⁻⁴
3.3	-1.120×10 ⁻³	-6.103×10 ⁻⁴	-3.674×10 ⁻⁴	-5.158×10 ⁻⁴
3.4	-1.016×10 ⁻³	-5.050×10 ⁻⁴	-2.879×10 ⁻⁴	-4.054×10 ⁻⁴
3.5	-9.164×10 ⁻⁴	-4.155×10 ⁻⁴	-2.243×10 ⁻⁴	-3.170×10 ⁻⁴
3.6	-8.207×10 ⁻⁴	-3.399×10 ⁻⁴	-1.738×10 ⁻⁴	-2.469×10 ⁻⁴
3.7	-7.311×10 ⁻⁴	-2.764×10 ⁻⁴	-1.341×10 ⁻⁴	-1.916×10 ⁻⁴
3.8	-6.481×10 ⁻⁴	-2.233×10 ⁻⁴	-1.031×10 ⁻⁴	-1.482×10 ⁻⁴
3.9	-5.721×10 ⁻⁴	-1.792×10 ⁻⁴	-7.903×10 ⁻⁵	-1.144×10 ⁻⁴
4.0	-5.030×10 ⁻⁴	-1.428×10 ⁻⁴	-6.045×10 ⁻⁵	-8.826×10 ⁻⁵
4.1	-4.404×10 ⁻⁴	-1.130×10 ⁻⁴	-4.621×10 ⁻⁵	-6.803×10 ⁻⁵
4.2	-3.842×10 ⁻⁴	-8.876×10 ⁻⁵	-3.536×10 ⁻⁵	-5.250×10 ⁻⁵
4.3	-3.338×10 ⁻⁴	-6.920×10 ⁻⁵	-2.716×10 ⁻⁵	-4.064×10 ⁻⁵
4.4	-2.889×10 ⁻⁴	-5.358×10 ⁻⁵	-2.101×10 ⁻⁵	-3.163×10 ⁻⁵
4.5	-2.490×10 ⁻⁴	-4.123×10 ⁻⁵	-1.642×10 ⁻⁵	-2.484×10 ⁻⁵
4.6	-2.137×10 ⁻⁴	-3.158×10 ⁻⁵	-1.303×10 ⁻⁵	-1.974×10 ⁻⁵
4.7	-1.827×10 ⁻⁴	-2.412×10 ⁻⁵	-1.054×10 ⁻⁵	-1.593×10 ⁻⁵
4.8	-1.556×10 ⁻⁴	-1.843×10 ⁻⁵	-8.729×10 ⁻⁶	-1.310×10 ⁻⁵
4.9	-1.319×10 ⁻⁴	-1.412×10 ⁻⁵	-7.404×10 ⁻⁶	-1.099×10 ⁻⁵
5.0	-1.114×10 ⁻⁴	-1.091×10 ⁻⁵	-6.436×10 ⁻⁶	-9.428×10 ⁻⁶

the matrix elements going through zero in this region, as indicated by the form factors in Table I. As in the case of zinc, the logarithmic singularity in $E(q)$ at exactly $2k_F$ is not visible on the scale to which the plot is made. Finally, it is noted that the decay at large q is more rapid for aluminum than for magnesium and sodium. The decay has been followed out to $9k_F$ in aluminum and shows an additional decrease in $E(q)$ of a factor of 40 below that at $5k_F$. In the calculations of properties we have made, the convergence of the sums to large q has been quite rapid. Had we not separated the electrostatic energy, but included its effect in $E(q)$, the decay would have been only as $1/q^2$, and the convergence very bad.

As we did for zinc,² we may add the band-structure and electrostatic energy and Fourier transform to obtain the effective two-body central force interaction between ions. This has been done for aluminum and the result shown in Fig. 3. There is some drift in the curve at large r arising from slight inaccuracy in $E(q)$ at small q . The drift was much worse for magnesium and sodium and these curves are not shown. Pick¹⁷ has compared the amplitude and frequency of these oscillations and finds they are very close to the asymptotic oscillations which arise from the logarithmic singularity in $E(q)$ at $q=2k_F$. This is rather surprising, since the singularity itself is

¹⁷ R. Pick (private communication).

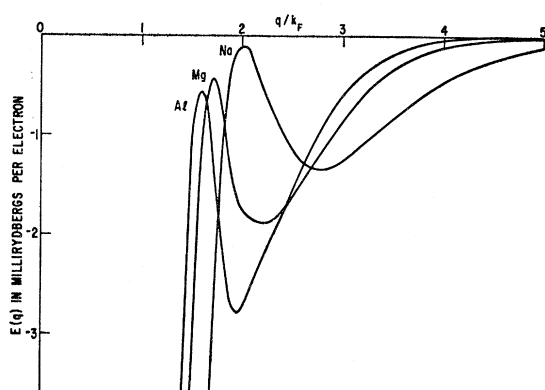


FIG. 2. The computed energy-wave-number characteristics $E(q)$ for sodium, magnesium, and aluminum, each at the observed atomic volume.

not visible; however, it suggests that the associated distortions of $E(q)$ in this region are the source of the oscillations rather than the peak which comes from the vanishing of matrix elements. In any case, for the computation of properties we have found it much more convenient to use the $E(q)$ curves of Table II directly.

We should perhaps also mention, in connection with Fig. 3, that the existence of this central-force interaction does *not* imply that the elastic constants will satisfy the Cauchy relations, because there is an additional volume-dependent term. Thus, the ions are not in equilibrium positions with respect to the central-force interaction by itself, a condition which is required for the derivation of the Cauchy relations.

IV. COMPUTATION OF PROPERTIES

The first use of the $E(q)$ curves we make is the comparison of the energy of different crystal structures. We have done this for the three simple metallic structures—

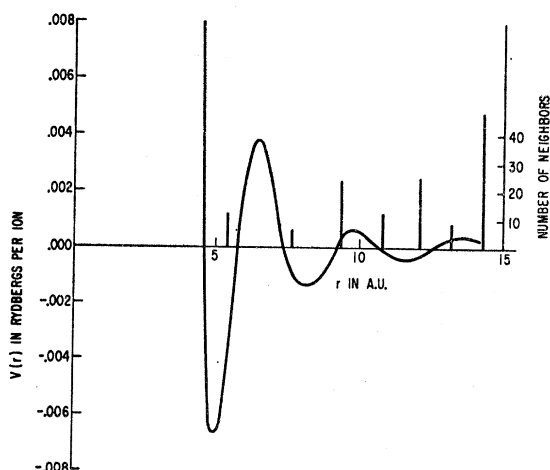


FIG. 3. The effective interaction between ions in aluminum. Also shown is the distribution of neighbors as a function of distance in the face-centered-cubic structure.

face-centered cubic, body-centered cubic, and hexagonal close-packed, the latter being carried out as a function of the axial ratio. In all cases the calculations were carried out at the observed atomic volume. The calculations are straightforward; we construct the reciprocal lattice, evaluate the structure factor $S(\mathbf{q})$ and the appropriate $E(q)$ for each and sum over the reciprocal lattice to obtain the band-structure energy. It is interesting to note that it is necessary to sum over a rather large number of reciprocal lattice vectors before the sum settles down. Figure 4 shows the sum for body-centered and hexagonal close-packed structures in comparison to the sum for face-centered cubic as reciprocal lattice vectors within a larger and larger sphere are included. A large portion of the oscillation arises because of a different total number of reciprocal lattice vectors within a given sphere for the different structures. This means that to distinguish the energies of the different

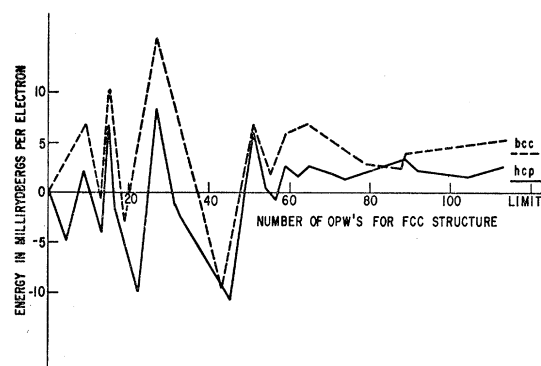


FIG. 4. Convergence of the energy summation in aluminum. The curves represent the difference in band-structure energy between hexagonal-close-packed (solid line) or body-centered-cubic (dashed line) and that for face-centered-cubic as a function of the volume of wave number space over which we had summed. The limiting values shown are for summation over several hundred reciprocal lattice vectors.

structures, a very complete description of the electronic states is needed—in fact, one involving well over 50 orthogonalized plane waves. In our calculations we sum over several hundred reciprocal lattice vectors and note that fluctuations are smaller than a part in a thousand. In these calculations, $E(q)$ was interpolated by fitting a cubic equation to values at the four nearest q 's given in Table II.

The electrostatic energy for each structure appears in the literature.¹⁸ These values have been obtained by Ewald sum methods. However, a value for the hexagonal-close-packed structure appears only for the ideal axial ratio. In our treatment of zinc we used Huntington's¹⁹ computation of a shear constant to estimate the

¹⁸ W. J. Carr, Jr., *Phys. Rev.* **122**, 1437 (1961).

¹⁹ H. B. Huntington, in *Solid State Physics*, edited by F. Seitz and D. Turnbull (Academic Press Inc., New York, 1958), Vol. 7, p. 213.

TABLE III. Electrostatic energy. The energy per ion is given by $Z^2\alpha/r_0$ rydbergs where Z^* is the effective valence, r_0 is the atomic sphere radius in atomic units, and α is

fcc	-1.79172 ^a
bcc	-1.79186 ^a
hcp	
axial ratio	
1.633	-1.79168 ^b
1.5	-1.78998
1.6	-1.79156
1.7	-1.79129
1.8	-1.78909
1.9	-1.78497
2.0	-1.77892

^a K. Fuchs, Proc. Roy. Soc. (London) A151, 585 (1935).^b W. Kohn and D. Schechter (unpublished). Result quoted by Carr (Ref. 18).

values for other axial ratios. Here we evaluate them accurately. We write the energy as the sum over reciprocal space for general axial ratio and formally perform the summations in a way to give an exponentially convergent sum over reciprocal lattice vectors in the basal plane. There remains an undetermined constant term which may be evaluated by fitting the energy obtained by Kohn and Schechter²⁰ at the ideal axial ratio. The results of this calculation are given in Table III.

Thus we obtain the energy for each metal for the various crystal structures. Table IV gives these values; for the hexagonal structure we give the axial ratio at which the minimum energy occurs and that energy. The electrostatic energy used is the difference between the computed electrostatic energy and that for a point ion in an atomic sphere [corresponding to a value of α (see Table III) of -1.8]. The correct structure is obtained in each case, though it must be admitted that the difference in energy found between hexagonal and face-centered-cubic sodium is perhaps too small to be regarded as significant. The computed axial ratios, also, are very close to those observed in sodium and magnesium and

TABLE IV. Energy of the crystal structures in rydbergs per ion.

	Na	Mg	Al
Face-centered cubic			
Band structure	-0.03797	-0.11412	-0.22275
Electrostatic	+0.00240	+0.01172	+0.02907
Total	-0.03557	-0.10240	-0.19368
Body-centered cubic			
Band structure	-0.03759	-0.11192	-0.20835
Electrostatic	+0.00236	+0.01152	+0.02859
Total	-0.03523	-0.10040	-0.17976
Hexagonal close packed			
Band structure	-0.03802	-0.11650	-0.22725
Electrostatic	+0.00241	+0.01182	+0.03729
Total	-0.03561	-0.10468	-0.18996
c/a	1.629	1.619	1.793
c/a (observed)	1.634 ^a	1.630	...

^a C. S. Barrett, Acta Cryst. 9, 671 (1956).²⁰ W. Kohn and D. Schechter (unpublished), quoted in Ref. 18.TABLE V. A shear constant in the hexagonal phase $C_{11}+C_{12}+2C_{33}-4C_{13}$ in units of 10^{11} dyn/cm².

	Na	Mg	Al
Band structure	-0.79	-17.8	-106.2
Electrostatic	+3.55	+30.0	+117.6
Total	2.76	12.2	11.4
Experimental	...	12.3 ^a	...

^a R. E. Schmunk and C. S. Smith, Phys. Chem. Solids, 9, 100 (1959).

to the ideal value of 1.633. It is striking that the axial ratio for hexagonal aluminum is somewhat higher.

The computed difference in energy between body-centered and hexagonal sodium (5×10^{-3} eV/atom) is somewhat higher than the experimental estimate given by Martin²¹ (0.15×10^{-3} eV/atom). Such a discrepancy might arise partly from our calculation being at constant volume, while experimentally there is an appreciable change in volume during the transition. In addition, it is very difficult experimentally to obtain parameters for a system which only partially transforms and for which the degree of transformation is not directly measurable. We therefore do not feel that this comparison gives a real measure of our error. The fact that the face-centered energy lies between the other two is not unreasonable. Presumably it is just the body-centered lattice which is soft and which therefore has a rapidly increasing entropy with temperature such that the free energy soon becomes lower than that for the hexagonal structure. We note that in magnesium the energy difference is an order of magnitude bigger and the transformation is therefore suppressed.

In computing the energy as a function of axial ratio, we also obtain directly the elastic shear constant associated with this distortion. The values so obtained are given in Table V. The agreement with experiment for magnesium is even closer than the precision of our calculations. Though the elastic constant for sodium is not known, we may expect our computed value is rather close since it is close to the electrostatic value (which would be 3.1×10^{11} dyn/cm² for a unit effective charge). The electrostatic energy is known to give a good account of the elastic constants in body-centered sodium.²² The striking thing about the aluminum result is the extremely strong cancellation between electrostatic and band-structure contributions. The result that the cancellation between electrostatic and band-structure terms grows rapidly from sodium to aluminum could have been reached by considering just the electrostatic and experimental elastic constants. For testing our theory it is an important fact to keep in mind; comparisons with sodium do not provide a very stringent test, but any errors in our band-structure calculation for aluminum can be greatly magnified in the results. It is aluminum which provides the most sensitive test.

²¹ D. L. Martin, Proc. Roy. Soc. (London) A254, 433 (1960).²² Reference 19, p. 288.

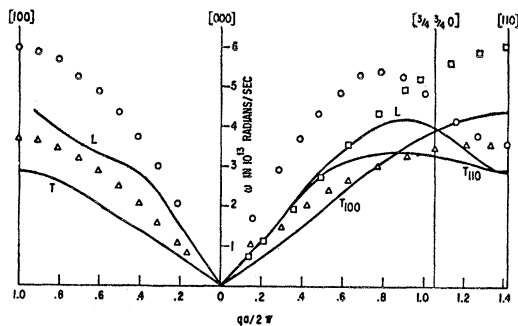


FIG. 5. Computed vibration spectrum of aluminum compared with the experimental spectrum determined by J. L. Yarnell, J. L. Warren, and S. H. Koenig, Proceedings of the International Conference on Lattice Dynamics, Copenhagen, August 1963 (published in Phys. Chem. Solids).

For this reason, it is of particular interest to consider the more complete set of distortions in aluminum represented by the vibration spectrum. The dispersion curves have been computed for face-centered cubic aluminum for propagation along the $[100]$ and $[110]$ directions; the results are plotted in Fig. 5 along with the experimental results. This could scarcely be called good quantitative agreement with experiment. However, we should keep in mind first that except for the use of the observed atomic volume, no experimental parameters enter the calculation, and there is no opportunity to include successive terms until agreement is reached. Second, aluminum provides a very sensitive test because of the strong cancellation. The comparison with experiment represents rather good agreement for the band-structure energy, as may be seen from comparison of the elastic constants derived from Fig. 5 with those based solely on electrostatic energy and with those obtained from experiment. This comparison is made in Table VI. The error for the fundamental shear constant c_{44} is a factor of 2, but because of the strong cancellation this represents an error in the band-structure contribution to the energy of less than 10%. The error in the small band-structure energy contribution for the other shear constant is greater than a factor of 3; it is interesting to note that in this one case, we find the band structure effects increasing the stiffness, as we should.

Although this calculation is restricted to constant total volume, we obtain a value for the bulk modulus. We note that the bulk modulus derived from our com-

TABLE VI. Elastic constants in aluminum in units of 10^{11} dyn/cm².

	Shear c_{44} ($c_{11} - c_{12}$)/2		Longitudinal c_{11} ($c_{11} + c_{12} + 2c_{44}$)/2		Bulk $(c_{11} + 2c_{12})/3$
Electrostatic	17.2	1.8
Total	1.5	3.4	6.0	4.1	1.5
Experimental ^a	2.8	2.3	10.7	11.2	7.6

^a R. E. Schumck and C. S. Smith, Phys. Chem. Solids 9, 100 (1959).

puted vibration spectrum is in error by a factor of 5, which is partially responsible for the errors in the longitudinal elastic constants. We may also note that this error in the bulk modulus gives rise to a negative value of c_{12} , contrary to experiment. We cannot compare the longitudinal constants with electrostatic values, since the latter diverge; however, we can compare them with the Bohm-Staver²³ value for both longitudinal constants, which is 23 for aluminum based upon an effective charge of three.

We have made a further calculation which provides a check upon the internal consistency of the theory; this is the calculation of the conduction-electron density in the crystal. Since it was necessary to compute the first-order screening field in the course of our calculation, we may also readily compute the first-order conduction-electron charge density. This has been computed for face-centered-cubic aluminum and added to a uniform density, with the result shown in Fig. 6. The density plotted includes the increase outside the core due to renormalization after orthogonalization, but not the orthogonalization charge itself; thus, a more complete calculation would give a further lowering in density at the cores. The decrease in density at the cores is overestimated in any case, since we find negative electron densities at those points. Except at the cores, the charge density is found to be rather uniform, varying from 0.63 to 1.38 times the average. This supports our treatment of the first-order terms in the wave functions as small and therefore supports, to some extent, our use of perturbation theory. Similar calculations for aluminum and silicon²⁴ in a diamond structure show strong non-uniformity and therefore appreciable unreliability of the perturbation expansion.

V. VOLUME-DEPENDENT PROPERTIES

We proceed next to the variation of energy with volume and therefore the inclusion of the free-electron energy E_{fe} . We have computed the energy-lattice-wave-number characteristic as well as the free-electron

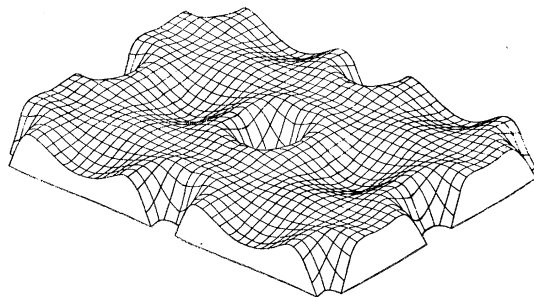


FIG. 6. Conduction electron density on a (110) plane in aluminum. This is a projection of a three-dimensional plot; if viewed from above, the lines would form a square grid.

²³ D. Bohm and T. Staver, Phys. Rev. 84, 836 (1950).

²⁴ W. A. Harrison (to be published).

TABLE VII. Total binding energy computed for aluminum in rydbergs per ion.

	Compressed	Observed density	Expanded
k_f	1.0200	0.9273	0.8346
E_{fe}	4.513	3.453	2.597
E_{be}	-0.319	-0.223	-0.201
E_{ee}	-7.408	-6.370	-5.479
Total	-3.214	-3.140	-3.083
Exch. and corr.	-1.692	-1.522	-1.355
Total	-4.906	-4.662	-4.438

energy and the electrostatic energy for aluminum for higher density, such that k_F was increased by 10%, and lower density, such that k_F was decreased by 10%, as well as at the observed density. The total binding energies (energy of the metal minus the energy of isolated ions and isolated electrons) obtained from these calculations for face-centered-cubic aluminum are given in Table VII. The final numbers, which include correction for exchange and correlation, will be discussed in the following section.

The agreement with the observed binding energy of 4.16 Ry per ion is certainly not good though we will see that it is improved by the addition of the correction for exchange and correlation. Furthermore, the energy continues to drop as the volume drops rather than showing a minimum at the observed density. This difficulty will not be ameliorated by the inclusion of an exchange and correlation correction.

These results look particularly unsatisfactory when compared with the computations by Brooks⁹ on the cohesive energy and lattice distance of a number of metals. He found a discrepancy of only about 0.01 Ry for aluminum and good agreement with the lattice distance. Two particular differences in the approaches may explain the differences in results. First, Brooks was able to deal directly with the small cohesive energy (0.24 Ry) rather than the total binding energy. Second, he used the quantum defect method to obtain the interaction of the electrons with the ions, and thereby used an experimental interaction rather than one computed from first principles. In any case, the approach used by Brooks appears much more informative with respect to the total energy and its change with volume, and we conclude that our computation of the free-electron energy is not accurate enough to be useful.

We may, however, consider two volume-dependent effects which do not depend upon our computation of the free-electron energy. These are the variation in the energy difference for the different metallic structures and the variation of the vibration spectrum with volume. Both of these are directly obtainable from the energy-lattice-wave-number characteristics which we computed for aluminum at the three volumes. The energy difference between structures is given in Table VIII. The axial

TABLE VIII. The energy of bcc and hcp structures minus that of the fcc structure in Al in rydbergs per ion.

	Compressed	Observed density	Expanded
k_f (a.u.)	1.0200	0.9273	0.8346
bcc	0.00738	0.00464	0.00204
hcp	0.00242	0.00124	-0.001
Axial ratio	1.684	1.793	>2.3

ratio for the hexagonal close-packed structure was carried out only to 2.3, so the numbers given for the expanded lattice are quite crude. Such a high ratio in the expanded aluminum would suggest that some other, and probably nonmetallic, structure would have lower energy. We note also the tendency of the fcc structure to become more stable at high pressure.

The vibration spectrum was computed at all three densities. In the expanded face-centered-cubic lattice, the crystal was unstable against the formation of almost all phonons propagating in the two directions computed, again reflecting the instability we found above. In the compressed lattice, the frequencies of all modes were roughly doubled. We may use these changes in frequency to estimate the pressure derivatives of the elastic constants; that is, we approximate $dC/d \ln r$ by $r_0 \delta C / \delta r_0$. The results are given in Table IX along with the experimental values from Schmunk and Smith.

VI. FREE-ELECTRON EXCHANGE AND CORRELATION

Our treatment of exchange and correlation is that proposed by Brooks⁹ and is simply a generalization of Slater's⁸ free-electron exchange. Gell-Mann and Brueckner²⁵ have given the energy of a free-electron gas as a function of electron density in the high-density limit. We may formally write this result as a density-dependent (uniform) self-consistent potential equal to twice the Gell-Mann-Brueckner expression. When we compute the total energy we subtract the electron-electron interaction including this self-consistent potential, which has been counted twice, to obtain the correct result. This is generalized to nonuniform electron densities simply by letting the self-consistent potential depend upon position through the dependence of the density upon position. The necessity of the factor of 2 is made clear physically by considering a variational argument; as we

TABLE IX. Pressure derivatives of the elastic constants, $dc/d \ln r$, in aluminum in 10^{11} dyn/cm².

	c_{44}	$(c_{11} - c_{12})/2$	$(c_{11} + 2c_{12})/3$
Theoret.	-90	-70	-100
Exptl. ^a	-50.4	-35.3	-114

^a R. E. Schmunk and C. S. Smith, Phys. Chem. Solids 9, 100 (1959).

²⁵ M. Gell-Mann and K. A. Brueckner, Phys. Rev. 106, 364 (1957).

change the position of a single electron, the energy of the entire system changes because of the change in energy of that electron and because of the change in energy of the electrons it interacts with. These changes are equal and add.

In our calculation of the free-electron energy, only the uniform potential enters and we may use the Gell-Mann-Brueckner expression directly. In computing the band-structure energy we treat the first-order fluctuations in charge density as small. Thus in going from the Hartree treatment to that including free-electron exchange and correlation, we simply replace the Poisson equation (which enters the calculation of the self-consistent field) relating a Fourier component of the interaction potential $v_{q^{sc}}$ to a Fourier component of the electron density ρ_q by the equation

$$v_{q^{sc}} = [4\pi e^2/q^2 + 2(dE^{e+c}/d\rho)]\rho_q, \quad (19)$$

where

$$E^{e+c} = -0.916/r_s + 0.0622 \ln r_s - 0.096$$

and

$$\rho = 3/(4\pi r_s^3).$$

Poisson's equation is given by Eq. (19) with the term in E^{e+c} dropped.

This treatment is equivalent by definition to the high-density expression for treating the uniform component of the charge density and should be good also for long wavelengths. It becomes quite suspect, however, for wavelengths of the order of r_s . In treating perfect crystals the smallest wave numbers which enter correspond to reciprocal lattice vectors, where this condition is already reached. Thus, at best, it is a very crude method for including exchange and correlation in the calculation of $E(q)$. One might well expect Hubbard's method¹⁰ as used by Sham¹¹ to be preferable for large wave numbers.

In Table VII we showed the effect of adding free-electron correlation and exchange to the free-electron energy as a function of volume.²⁶ This brings the binding energy into better agreement with experiment (4.16 Ry/ion), but does not bring the minimum energy any closer to the observed spacing.

The inclusion of free-electron exchange and correlation in the band-structure energy does not seem to improve the situation. This has been done only at the observed volume and was found to lower the energy by another tenth of a rydberg per ion, worsening the agreement with experiment.

Finally, we computed the vibration spectrum from the $E(q)$ curve which included free-electron exchange and correlation. It was found that the lattice became unstable against the formation of almost all phonons considered (those shown in Fig. 5).

We can only conclude that the inclusion of this simple correction for exchange and correlation worsens our

²⁶ Here the density used was the electron density between ions; that is, the renormalized density. The average density would perhaps be more appropriate but the difference is small.

agreement with experiment. Only in the total energy are the results improved, and these are very inaccurate in any case.

VII. A PHENOMENOLOGY BASED UPON THE THEORY

Our discussion up to this point has concerned an attempt to compute known properties of metals from first principles. Physical and mathematical approximation have been used, but no experimental parameters have been introduced. We noted that there was an arbitrariness in the pseudopotential which is reflected in the arbitrary function $f(\kappa, \alpha)$, which we removed by attempting to optimize the convergence of the perturbation expansion. We could instead adjust $f(\kappa, \alpha)$ to obtain agreement with some experimental findings and thereby obtain a phenomenological $E(q)$ which hopefully would describe other experiments.

The success we have had in treating a number of properties would suggest that the $f(\kappa, \alpha)$ which we have obtained from the theory is rather close to the best one and would suggest that we proceed by adding experimental corrections to our computed $f(\kappa, \alpha)$. The simplest such correction is the addition of a constant. We have sought to optimize the agreement with the vibration spectrum in aluminum with the addition of a constant. The result is shown in Fig. 7 based upon an $E(q)$ [the phenomenological $E(q)$ given in Table II] which was calculated by adding 0.64 Ry to the $f(\kappa, \alpha)$ from the theory. The agreement is perhaps not remarkable, but one should keep in mind that only a single adjustable parameter has been introduced. It should also be noted that this calculation also corresponds to a *correct* pseudopotential in the sense that exact solution of the pseudopotential equation should lead to exactly the same energy bands as with the other pseudopotential or with our starting Hamiltonian. It might finally be noted that the addition of this constant raises the value of the form factors of Table I by roughly 0.02 Ry.

The important consideration concerning the development of a phenomenology is that the results of calcula-

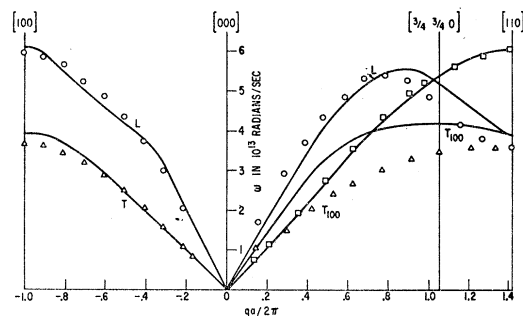


FIG. 7. Vibration spectrum of aluminum from the phenomenological calculation based upon a single adjustable parameter. Comparison is made with the measurements of J. L. Yarnell, J. L. Warren, and S. H. Koenig, Proceedings of the International Conference on Lattice Dynamics, Copenhagen, August 1963 (published in Phys. Chem. Solids).

tions will depend upon the particular formulation. A complete knowledge of the vibration spectrum does not contain sufficient information for computing all properties. This is most clearly seen in terms of the effective ion-ion interaction of Fig. 3; this is the Fourier transform of $E(q)$ (plus a simple Coulomb term). The vibration spectrum is determined entirely by the first and second derivatives of this curve evaluated *only* at the observed interatomic spacings. Thus any curve which fits these derivatives fits the vibration spectrum but each will lead to different results for other properties. The missing information must be supplied by the form of the phenomenology. It is therefore important to base the phenomenology upon a theory which gives a good account of a range of properties of the material in its own right.

APPENDIX

We will proceed with the evaluation of the matrix elements of W , which we obtain from Eq. (15),

$$W|\mathbf{k}\rangle = V|\mathbf{k}\rangle + \sum_{\alpha} (\hbar^2 k^2 / 2m + \langle \mathbf{k}|W|\mathbf{k}\rangle - E_{\alpha}) |\alpha\rangle \langle \alpha|\mathbf{k}\rangle, \quad (\text{A1})$$

and will finally evaluate the total energy. We first eliminate the appearance of W upon the right-hand side by multiplying on the left by $\langle \mathbf{k}|$, solving for $\langle \mathbf{k}|W|\mathbf{k}\rangle$, and substituting back into Eq. (A1) to obtain

$$W|\mathbf{k}\rangle = U|\mathbf{k}\rangle + \frac{\langle \mathbf{k}|U|\mathbf{k}\rangle P|\mathbf{k}\rangle}{1 - \langle \mathbf{k}|P|\mathbf{k}\rangle}, \quad (\text{A2})$$

where

$$U|\mathbf{k}\rangle = V|\mathbf{k}\rangle + \sum_{\alpha} (\hbar^2 k^2 / 2m - E_{\alpha}) |\alpha\rangle \langle \alpha|\mathbf{k}\rangle. \quad (\text{A3})$$

We may note that U is a first-order quantity; but, since $\hbar^2 k^2 / 2m$ is a zero-order quantity, Eq. (A3) indicates that P must also be regarded as first order. This is satisfactory since $\langle \mathbf{k}|P|\mathbf{k}\rangle$ is of the order of 0.1; however, it means that our use of W in the form of Eq. (A1) will mean that selected higher order terms will appear in our "second-order" energy of Eq. (13). This need not worry us, but we may note that the use of the potential of Pick and Sarma⁴ (their pseudopotential is simply U) could be justified as retaining only true second-order terms.

The potential V entering our pseudopotential is to be the self-consistent potential and therefore includes the potential due to the conduction electrons. This latter contribution includes a zero-order term coming from plane-wave electrons, a first-order term (because $\langle \mathbf{k}|P|\mathbf{k}\rangle$ is first order) from orthogonalization and renormalization, and a first-order term from the use of first-order terms in the wave function with coefficients given by Eq. (12). This final term is the screening field; in computing it we may again treat the orthogonalized plane waves as plane waves to obtain the first-order result. Second-order terms in V could only enter a second-order energy calculation through $\langle \mathbf{k}|V|\mathbf{k}\rangle$, but

there is no screening of the diagonal terms. The first-order screening terms are obtained by summing over occupied electron states in just the way we will sum over states to obtain the total energy.

The only remaining ambiguity is in the evaluation of E_{α} . In our treatment of a series of metals³ and in Sham's treatment of the sodium vibration spectrum,¹¹ E_{α} was taken equal to the eigenvalue of the free ion. This is again an allowed pseudopotential, but in line with our attempt to make $f(\mathbf{r}, \alpha)$ as close to $E_k - E_{\alpha}$ as possible (and also to give the optimized pseudopotential mentioned earlier) we wish to take E_{α} to be the core eigenvalue in the metal. We distinguish between the evaluation of the diagonal element $\langle \mathbf{k}|W|\mathbf{k}\rangle$ and the off-diagonal elements entering the second-order sum.

The diagonal term is given by

$$\begin{aligned} \langle \mathbf{k}|W|\mathbf{k}\rangle &= \langle \mathbf{k}|U|\mathbf{k}\rangle / (1 - \langle \mathbf{k}|P|\mathbf{k}\rangle) \\ &= \langle \mathbf{k}|V|\mathbf{k}\rangle \\ &\quad + \sum_{\alpha} \frac{(\hbar^2 k^2 / 2m + \langle \mathbf{k}|V|\mathbf{k}\rangle - E_{\alpha}) \langle \mathbf{k}|\alpha\rangle \langle \alpha|\mathbf{k}\rangle}{1 - \langle \mathbf{k}|P|\mathbf{k}\rangle}. \end{aligned} \quad (\text{A4})$$

E_{α} appears multiplied by $\langle \mathbf{k}|P|\mathbf{k}\rangle$; thus we need E_{α} to first order. To first order it is given by the eigenvalue in the isolated ion plus the potential evaluated at the nucleus due to (a) the tails of the ion potentials from other ions, plus the field due to their orthogonalization charges (that is, the charge induced at each ion by orthogonalizing the plane waves to the core states on that ion); (b) the potential due to a uniform compensating negative background; (c) the potential due to the orthogonalization charge at the ion in question; and (d) the screening field due to the use of first-order wave functions for the conduction electrons. The terms (a) and (b) combine naturally with $\langle \mathbf{k}|V|\mathbf{k}\rangle$ and with the direct electrostatic interaction between the ions to give a modified effective charge for the electrostatic energy. The term (c) is the same for all ions and may be evaluated at the beginning; it is of the order of a rydberg in the metals we treat. The term (d) combines naturally with the band-structure energy when we compute the total energy.

The off-diagonal matrix elements of W may be conveniently obtained by combining Eqs. (A2) and (A3) and writing the result in the form,

$$\begin{aligned} \langle \mathbf{k}+\mathbf{q}|W|\mathbf{k}\rangle &= \langle \mathbf{k}+\mathbf{q}|V|\mathbf{k}\rangle \\ &\quad + \sum_{\alpha} \langle \mathbf{k}+\mathbf{q}|\hbar^2 k^2 / 2m + \langle \mathbf{k}|V|\mathbf{k}\rangle \\ &\quad - E_{\alpha} |\alpha\rangle \langle \alpha|\mathbf{k}\rangle + \sum_{\alpha} \langle \mathbf{k}|\frac{\hbar^2 k^2}{2m} + \langle \mathbf{k}|V|\mathbf{k}\rangle \\ &\quad - E_{\alpha} |\alpha\rangle \frac{\langle \alpha|\mathbf{k}\rangle \langle \mathbf{k}+\mathbf{q}|P|\mathbf{k}\rangle}{1 - \langle \mathbf{k}|P|\mathbf{k}\rangle}. \end{aligned} \quad (\text{A5})$$

Again we consider the four corrections to the value of E_α for the isolated ion which we listed in the previous paragraph. The contributions (a) and (b) may be combined with terms in $\langle \mathbf{k} | V | \mathbf{k} \rangle$ to give an energy closely related again to the electrostatic energy of point ions in a uniform negative background. Since this electrostatic energy is almost exactly equal to that obtained by replacing each atomic cell by a uniform isolated sphere with volume equal to the atomic volume, and since we require a value averaged over all ions, we evaluate these terms by making that replacement. The term (c) is evaluated as for the diagonal terms, and the term (d) is dropped. This term (d) is a second-order term in W which in fact depends upon the arrangement of the ions; a numerical examination of this correction in aluminum indicated that it is in fact tiny in comparison to the other corrections. We obtain finally a value for $\langle \mathbf{k} | V | \mathbf{k} \rangle - E_\alpha$ given by

$$\langle \mathbf{k} | V | \mathbf{k} \rangle - E_\alpha \approx \frac{3}{r_0^3} \int_0^{r_0} v^0(r) r^2 dr - \frac{3Ze^2}{10r_0} - \epsilon_\alpha - v_{\text{opw}}. \quad (\text{A6})$$

Here r_0 is the radius of a sphere containing an atomic volume, $v^0(r)$ is the potential within an isolated ion (including the Slater exchange potential), and v_{opw} is the potential at an ion due to the orthogonalization charge at that ion; ϵ_α is the Hartree-Fock energy parameter for the core level in question in the isolated ion.

We have now written all of the needed expressions in explicit forms which may be evaluated directly in terms of the potentials for isolated ions. We may proceed in the manner used earlier¹ to obtain the total energy.

We first decompose the index α into an index j specifying the ion and an index t specifying the core level in that ion. The total volume Ω is also factored into the number of ions N times the atomic volume Ω_0 . We may then factor the matrix elements of P .

$$\langle \mathbf{k} + \mathbf{q} | P | \mathbf{k} \rangle = S(\mathbf{q}) \langle \mathbf{k} + \mathbf{q} | p | \mathbf{k} \rangle, \quad (\text{A7})$$

with

$$S(\mathbf{q}) = N^{-1} \sum_j e^{-i\mathbf{q} \cdot \mathbf{r}_j} \quad (\text{A8})$$

and

$$\langle \mathbf{k} + \mathbf{q} | p | \mathbf{k} \rangle = \sum_t \langle \mathbf{k} + \mathbf{q} | t \rangle \langle t | \mathbf{k} \rangle, \quad (\text{A9})$$

where

$$\langle \mathbf{k} + \mathbf{q} | t \rangle = \Omega_0^{-1/2} \int e^{-i(\mathbf{k} + \mathbf{q}) \cdot \mathbf{r}} \psi_t(\mathbf{r}) d\mathbf{r}. \quad (\text{A10})$$

We may also define an operator ep such that

$$\langle \mathbf{k} + \mathbf{q} | ep | \mathbf{k} \rangle = \sum_t \langle \mathbf{k} + \mathbf{q} | (\frac{\hbar^2 k^2}{2m}) + \langle \mathbf{k} | V | \mathbf{k} \rangle - E_\alpha | t \rangle \langle t | \mathbf{k} \rangle, \quad (\text{A11})$$

with $\langle \mathbf{k} | V | \mathbf{k} \rangle - E_\alpha$ given by Eq. (A6). Then the off-diagonal elements of W may also be factored in the form

$$\langle \mathbf{k} + \mathbf{q} | W | \mathbf{k} \rangle = S(\mathbf{q}) \langle \mathbf{k} + \mathbf{q} | w | \mathbf{k} \rangle \quad (\text{A12})$$

with

$$\langle \mathbf{k} + \mathbf{q} | w | \mathbf{k} \rangle = v_q + \langle \mathbf{k} + \mathbf{q} | ep | \mathbf{k} \rangle + \langle \mathbf{k} | ep | \mathbf{k} \rangle \langle \mathbf{k} + \mathbf{q} | p | \mathbf{k} \rangle / (1 - \langle \mathbf{k} | p | \mathbf{k} \rangle), \quad (\text{A13})$$

where the Fourier transform of the potential has also been factored

$$\langle \mathbf{k} + \mathbf{q} | V | \mathbf{k} \rangle = S(\mathbf{q}) v_q. \quad (\text{A14})$$

This factorization of the matrix elements will enable us to carry out the various integrations before specifying the arrangement of the ions and will thereby give us the total energy as a function of ion positions.

We proceed by summing the second-order energies of Eq. (13) over all states within the Fermi sphere. The difference between the sum over the unperturbed sphere and the true distorted Fermi surface is third order in W and therefore negligible. From this we subtract an energy equal to the Coulomb self-energy of the conduction electrons, which is counted twice in the Hartree approximation, and add the direct Coulomb interaction between the ions to obtain the total energy. The treatment of these electron self-energy terms and their combination with the contribution from the diagonal terms $\langle \mathbf{k} | W | \mathbf{k} \rangle$ is tedious but straightforward, and no additional approximations are necessary. Finally we decompose the energy into three parts. The free-electron energy per electron is given by

$$E_{fe} = \frac{3 \hbar^2 k_F^2}{5} \frac{1}{2m} \frac{1}{NZ} \sum_{k,t} \frac{(\epsilon_t + \frac{1}{2} v_{\text{opw}} - \hbar^2 k^2 / 2m) \langle \mathbf{k} | t \rangle \langle t | \mathbf{k} \rangle}{1 - \langle \mathbf{k} | p | \mathbf{k} \rangle} + \frac{1}{1 - \langle \mathbf{k} | p | \mathbf{k} \rangle_{\text{av}}} \int (v^0(r) - Ze^2/r) \frac{d\mathbf{r}}{\Omega_0} \quad (\text{A15})$$

and depends only upon the density of ions, not on their detailed arrangement. The band-structure energy per electron is written, taking advantage of the factorization of the matrix elements, in the form

$$E_{bs} = \sum_q S^*(\mathbf{q}) S(\mathbf{q}) E(q), \quad (\text{A16})$$

where

$$E(q) = \frac{1}{NZ} \sum_k \frac{|\langle \mathbf{k} + \mathbf{q} | w | \mathbf{k} \rangle|^2}{(\hbar^2 / 2m)(k^2 - (\mathbf{k} + \mathbf{q})^2)} - \frac{q^2 \Omega_0}{8\pi Z e^2} |v_q^{sc}|^2. \quad (\text{A17})$$

Here v_q^{sc} is the contribution of the first-order screening field to v_q . Finally, the electrostatic energy is equal to the electrostatic energy of point ions with a number of electronic charges equal to the effective valence,

$$Z^* = Z(1 + (NZ)^{-1} \sum_k \langle \mathbf{k} | p | \mathbf{k} \rangle) \quad (\text{A18})$$

embedded in a uniform compensating background.

In addition to a slightly different form of the matrix elements of w from the one we had in our previous treatment,¹ there is a difference in the decomposition of the energy into these three terms. In our earlier treatment, an additional term in $E(q)$ appeared which was proportional to w and to p . Pick and Sarma⁴ have shown that the application of the closure relation to this term puts

it in a form in which it can be naturally included partly in the free-electron energy and partly in the electrostatic energy. That term never appears explicitly in the present treatment because of our choice of a Hermitian w in Eq. (15). Thus, we now have a different effective charge for the electrostatic energy, which is equal to the charge

on the ion plus the orthogonalization charge at each ion. In addition, the free-electron energy is simpler in form. The separation given here, which is the same as that used by Pick and Sarma,⁴ seems much more natural than the one that we used earlier, though the total energy is the same in either case.

Knight Shifts and Susceptibilities of Transition Metals: Palladium*

J. A. SEITCHIK, A. C. GOSSARD, AND V. JACCARINO

Bell Telephone Laboratories, Murray Hill, New Jersey

(Received 17 June 1964)

The nuclear magnetic resonance (NMR) of Pd¹⁰⁵ has been observed for the first time. The temperature dependence of the Pd¹⁰⁵ NMR in palladium metal was studied in the region 1.4 to 300°K. The relatively large linewidth ($\delta H = 9 \pm 2$ Oe) at all temperatures necessitated the use of continuous averaging techniques to obtain the requisite sensitivity. The field for resonance, at a fixed frequency, was found to have a maximum in the vicinity of 85°K, as does the susceptibility $\chi(T)$. From an analysis of the temperature dependence of the Knight shift $K(T)$ and of $\chi(T)$ it was deduced that: (1) d -spin paramagnetism is responsible for the observed behavior of $K(T)$ and $\chi(T)$, (2) the principle contribution to K in Pd arises from d -spin-induced core polarization and (3) the core-polarization hyperfine field $H_{ep} = -689 \pm 20$ kOe/spin. From a partitioning of the various contributions to K , χ , and the specific heat, an estimated value of $1/T_1 \approx 0.8T \text{ sec}^{-1} \text{ }^\circ\text{K}$ is obtained for the nuclear spin-lattice relaxation rate at low temperatures. It is shown that the "knee" in $\chi(T)$ is *not* associated with a static antiferromagnetic ordering; an upper limit of $10^{-5} \mu_B$ per Pd atom for the spontaneous moment at low temperatures is obtained. A diamagnetically uncorrected value of the Pd¹⁰⁵ nuclear moment $\mu^{105} = -0.639 \pm 0.003$ nm was determined.

1. INTRODUCTION

THE large electronic specific heat C_e and susceptibility χ of palladium metal has been a subject of some interest for many years.¹⁻⁵ From AgPd alloying studies it has been advanced that the $4d$ band is shy 0.4 to 0.6 of an electron of being completely filled. The relatively large observed values of the electronic specific heat and the susceptibility have been associated with the combined effects of a large value of the density of states at the Fermi level in the d band $N_d(E_F)$ and a sizeable intraband exchange interaction.

Of particular interest is the behavior of the temperature dependence of χ , for it is found² that $\chi(T)$ exhibits a pronounced maximum in the vicinity of 85°K. This, and the fact that magnetic impurity studies have

shown⁶⁻⁸ Pd to be an extremely polarizable metal have quite naturally led to the belief⁹ that an ordered antiferromagnetic spin state occurs below 85°K. Alternatively it has been suggested⁴ that the anomalous peak in $\chi(T)$ could be obtained from an unusual shape to the density-of-states curves in the region of the Fermi level. Recent precise calorimetric measurements¹⁰ have shown there is no measurable specific-heat anomaly at the temperature corresponding to the maximum in $\chi(T)$ as would be expected from a second-order transition. In addition neutron diffraction measurements¹¹ have established that at low temperatures the spontaneous moment per Pd atom must be less than 0.03 Bohr magnetons. Observations of the nuclear magnetic resonance (NMR) of Pd¹⁰⁵ in Pd metal at low temperatures indicated that the upper limit on the magnetic moment per atom must be several orders of magnitude smaller than that which is deduced from the neutron experiments. (We will discuss the meaning of the latter two experiments later on.) Thus it appears there is little to support the conjecture of antiferromagnetism in Pd metal.

* A preliminary report of portions of this work has been given previously, A. C. Gossard and V. Jaccarino, *Bull. Am. Phys. Soc.* **7**, 556 (1962).

¹ N. F. Mott and H. Jones, *The Theory of the Properties of Metals and Alloys* (Clarendon Press, Oxford, England, 1936).

² F. E. Hoare and J. C. Matthews, *Proc. Roy. Soc. (London)* **A212**, 137 (1952); D. Budworth, F. Hoare, and J. Preston, *ibid.* **A257**, 250 (1960).

³ A. J. Manuel and J. M. P. St. Quinton, *Proc. Roy. Soc. (London)* **A273**, 412 (1963).

⁴ E. W. Elcock, P. Rhodes, and A. Teviotdale, *Proc. Roy. Soc. (London)* **A221**, 53 (1954).

⁵ M. Shimizu, *J. Phys. Soc. Japan* **16**, 1114 (1961). References to other theoretical work are given in this article.

⁶ F. W. Constant, *Phys. Rev.* **36**, 1654 (1930).

⁷ D. Gerstenberg, *Ann. Physik* **2**, 236 (1958).

⁸ J. Crangle, *Phil. Mag.* **5**, 335 (1960).

⁹ A. B. Lidiard, *Proc. Roy. Soc. (London)* **A224**, 161 (1954).

¹⁰ J. Crangle and T. F. Smith, *Phys. Rev. Letters* **9**, 86 (1962).

¹¹ S. C. Abrahams, *Phys. Chem. Solids* **24**, 589 (1963).